SCIENTIFIC REPORTS

OPEN

SUBJECT AREAS:
MEDICAL RESEARCH
CELL GROWTH

Received
13 November 2013

Accepted
31 March 2014

Published
22 April 2014

Correspondence and requests for materials should be addressed to T.D. (tulidey@yahoo.com) or S.C.K. (kundu@hijli.iitkgp.ernet.in)

Non-mulberry silk fibroin influence osteogenesis and osteoblast-macrophage cross talk on titanium based surface

Deboki Naskar, Sunita Nayak, Tuli Dey & Subhas C. Kundu

Department of Biotechnology, Indian Institute of Technology, Kharagpur-721302, India.

The titanium and its alloys are used as orthopedic dental implants due to their mechanical and bio-inert properties. The bare metal implants are not the ultimate answer for better osteogenesis and implant integration. Physical and chemical modifications are carried out to achieve the goal of improved adhesion and differentiation of the osteoblast. In this work, the silk fibroins from both mulberry and non-mulberry sources are used for surface modification. Silk fibroins are immobilized on titanium surface to facilitate the initial cell adhesion followed by improved cell spreading and better mineralization in order to achieve enhanced osseointegration. The immunological responses along with the effect of cytokines on osteoblast adhesion and function are investigated. The non-mulberry fibroin performs better in the context of the cell adherence and differentiation, which lead to better mineralization. The results indicate that the silk fibroin from non-mulberry source can be used for better osteogenesis on orthopedic implants.

The implant materials like titanium (Ti) and its different alloys (with Cr, Ni, Co, Al, V and others) are being used routinely for cardiac, dental and orthopedic applications[1] mostly due to their biocompatibility, mechanical strength and stability[2]. Never the less, orthopedic implants made from commercially pure Ti or Ti based alloys are found to be susceptible to certain obstacles such as inadequate cell adhesion, amplified immune response and implant mediated infections[3], which eventually lead to implant failure. It is reported that the fine (a few nanometer thick) layer of naturally produced titanium dioxide (TiO_2) on pure Ti implant surfaces provide the much needed bioactivity for cell attachment and bone-implant integration[4]. In most cases the inherent bioactivity is found to be inadequate to attain enough true bone-implant integration, which may initiate the poor osseointegration.

Initial cellular adhesion and formation of own extra cellular matrix on the implant surface are found to be a key step in implant integration followed by osseointegration or the anchorage of implant through bone tissue formation around the implant. Osteoconductive nature of the implant material surface controls the bone growth and future success of the implant. The implant surface is expected to support proper osseointegration and provide sufficient osteoconductivity for bone healing and regeneration[5]. To achieve essential osseointegration; surface charge, topography, and chemistry are subjected to the modification as the osteoconductivity of pure Ti implants is found to be limited[6].

Another key obstruction for long-term successful implant integration is nosocomial infection, which originates in the hospital. This problem can be circumvented by using local antibiotic delivery methods such as antibiotic loaded devices[7]. Elicited immune response against the implant surface also thwarts the osteogenesis process by secreting cytokines such as tumor necrosis factor alfa (TNF-α), interleukin beta (IL-1β) and nitric oxide (NO) which stimulate osteoclast generation and bone resorption. Previous report of direct co-culture of macrophage and osteoblast detects elevated TNF-α level against Ti micro particles[2]. Indirect co-culture study shows heightened level of TNF-α, IL-6, PGE_2 and GM-CSF level but no detectable IL-1β against rutile and pure Ti[8].

To decrease the immune response and to stimulate bone-Ti interactions, different approaches are carried out. Different techniques such as micro arc oxidation[9], laser ablation[10], sand blasting[11] and other methods[12] are employed to alter the surface topography. Surface chemistry modifications are carried out by hydroxyapatite deposition[13] or chemical treatment[14]. To attain the desirable Ti surfaces, surface modification is done by coating the surface with hydrophilic polymers such as chitosan[15]. However, according to the scientific body, the

biochemical characteristics of Ti surfaces may be modified by utilizing bioactive molecules such as peptides, or proteins to accomplish the mentioned challenges[16,17]. This involves chemical immobilization or physical deposition of the protein molecules such as bone morphogenic protein 2 (BMP2)[18], fibronectin[19], cyclo-DfKRG peptide[20] etc. for directional cell adherence. The chemical immobilization of protein or peptides through covalent modifications is used to obtain stable, uniform layer on Ti or implant surfaces.

As a natural biomaterial, silk protein fibroin obtained from silkworms of mulberry origin is found to be extremely useful in different biomedical applications[21] such as to prepare scaffold, thin film and other different types of matrices[22]. The silk fibroin offers significant promise as a biomaterial for bone tissue engineering[23] though *Bombyx mori* (Bm) fibroin does not contain osteogenic properties in itself[24]. Recent studies show the influence of cross linked RGD-fibroin[25,26] and RGD- sericin complex[27] on cellular adhesion and proliferation on Ti. The recent reports of non-mulberry fibroin from the species *Antheraea mylitta* (Am) show additional advantages due to its higher mechanical strength[28] and existence of integral RGD sequences[29]. Am fibroin is found to be greatly cytocompatible with lowered immune response[30], which supports the hypothesis of using it as an immobilizing agent in order to modify the chemical, physical and biological nature of the implant surface.

The present study utilizes the silk fibroins particularly non-mulberry fibroin as a viable material for Ti based implant surface modification. The biological effects of immobilized protein over osteoblast and macrophage activation are analyzed *in vitro* before designing any *in vivo* approach. For this reason the mulberry and non-mulberry silk protein fibroins are immobilized on titanium surfaces to evaluate their effects on osseointegration. The protein deposition is confirmed by FTIR, XPS and EDX analyses. The evaluations of adherence, growth, proliferation and differentiation of osteoblast like cells are carried out to determine the quality of osseointegration. To quantify the immune response of fibroin immobilized surfaces, TNF-α, IL1-β and nitric oxide production level are measured. The effect of cytokines on osteoblast adherence is analyzed by direct co-culture of macrophages and osteoblast. The result confirms the influence of silk protein fibroin particularly nonmulberry fibroin on the osteogenesis on modified titanium surface.

Results

Extraction of silk fibroin from mulberry (*Bombyx mori*/Bm) and non-mulberry tropical tasar (*Antheraea mylitta*/Am) sources. Mulberry silk (Bm) cocoon pieces (15.00 gm) yield 10.37 gm degummed fiber or fibroin (approx. 66%). Dissolution of the silk fiber in LiBr solution gives almost 100% yield of fibroin in solution form and finally a stock of 20 mg/ml is prepared. From non-mulberry tasar (Am) silk gland, obtained fibroin was dissolved in SDS solution. This was further diluted to reach 20 mg/ml stock.

For immobilization purpose 5 μl of 20 mg/ml of stock solution for each protein was used to reach a final concentration of 100 μg fibroin on each titanium coupon (1 cm^2).

Analysis of modified surface topography. The scanning electron microscopic (SEM) images of modified surfaces show that the surface topography is changed visibly following the immobilization of protein molecule compared to the non-treated surfaces (Fig. 1A). The chemical immobilization of protein molecules creates a uniform layer on Ti, without influencing the surface micro-roughness. Atomic force microscopic (AFM) observation shows immobilized protein molecules (Fig. 1B), altering the local nano-roughness compared to pristine Ti surface. The surface roughness index (quadratic roughness) is found to be 19.9 ± 1.05 nm in case of pristine Ti, 83.3 ± 7.6 nm for Bm and 114.23 ± 20.65 nm for Am, which show statistically significant differences ($p < 0.05$).

Analysis of modified surface chemistry. To study the changed chemistry of modified surfaces, quantitative analysis of element compositions are carried out by energy dispersive x-ray spectroscopy (EDX) and X-ray photoelectron spectroscopy (XPS). The comparative mapping of elements on the modified and the pristine Ti surfaces shows increased quantity of carbon, oxygen and nitrogen along with lowered Ti (Table 1). Fourier transform infra-red spectroscopy (FTIR) analysis of the modified Ti surfaces also indicates distinctive transmittance peak of amides A and B (N-H stretch) at 3100–3300 cm^{-1}, amide I (C=O stretch) at 1600–1700 cm^{-1} and amide II (N-H bend and C-N stretch) at 1510–1580 cm^{-1} in comparison with pure fibroin (Fig. 1C).

Analysis of osteoblast like cell adherence, proliferation, viability and spreading. Preliminary cell adherence efficiency of pristine and modified surface is measured by counting the nuclei of the attached cells after 4 h of seeding, which shows the efficiency of Am in comparison with other two surfaces (data not shown). The cell proliferation rates after 1st, 3rd and 5th day of seeding indicate that the modified Ti surfaces, specially the non-mulberry fibroin immobilized sample have significantly higher amount of proliferating cells in comparison to the pristine Ti on day 3 and 5 ($*p < 0.05$) (Fig. 2A).

The differences in cell viability and growth among the pristine and the modified Ti are visibly supported from the Live/Dead staining. The confocal images show maximum number of viable cells (green) on Am fibroin surface on day 3 (Fig. 2B). The Am fibroin coated surface supports the formation of actin stress fiber to control the cell spreading (Fig. 3A). The distribution of actin filament in Am coated surface is found to be different than of the pristine and Bm coated surfaces, where distinct contact dependent actin stress fiber like structure is not observed. The cell morphology of the three different surfaces (Fig. 3B) indicates that Am fibroin maintain the regular spindle shaped cellular morphology, which are connected to each other through well-developed filopodia in comparison to the pristine Ti and Bm immobilized surface.

Analysis of cellular functionality. Gene expression profiles of different osteogenic marker such as osteocalcin (OC) and alkaline phosphatase (ALP) show significant differences between Bm and Am fibroin samples (Fig. 4). Increased amount of osteocalcin and ALP mRNA on day seven indicates the earliest initiation of osteogenesis in Am fibroin immobilized surfaces. However the expression of integrin-binding sialoprotein (IBSP) on both time points does not differ significantly between the control and experimental samples.

Analysis of *in vitro* immune response against modified Ti surfaces. The protein coated surfaces show lower inflammatory response in terms of TNF-α and IL-1β secretion from macrophages after 24 hr (Fig. 5A–B). TNF-α level shows significantly increased amount in pristine Ti sample in comparison with modified samples. Il-1β secretion shows no significant differences between the control and experimental surfaces. Increased nitric oxide (NO) production from mono- and co-culture in all kinds of Ti surfaces on day 1 and 3, confirms the proliferating macrophage population (Fig. 5C–D).

Analysis of macrophage induced effect on osteoblast function. Direct co-culture model indicates much lower level of TNF-α, IL-1β and NO production in comparison to macrophage only culture (Fig. 5A–D), which may occur due to cellular cross-talk. In co-cultured samples the macrophages do not appear to thwart the preliminary adhesion of the osteoblast on fibroin specifically on Am immobilized surfaces as observed both in pre-stained cells and SEM images (Fig. 6A–B). The osteoblast adhesion is visibly reduced in the presence of macrophage on the pristine Ti surface. Rapid mineralization or calcium deposition is required to attain better integration of the implant. Qualitative detection of deposited calcium in co-cultured surfaces is carried out by Alizarin red

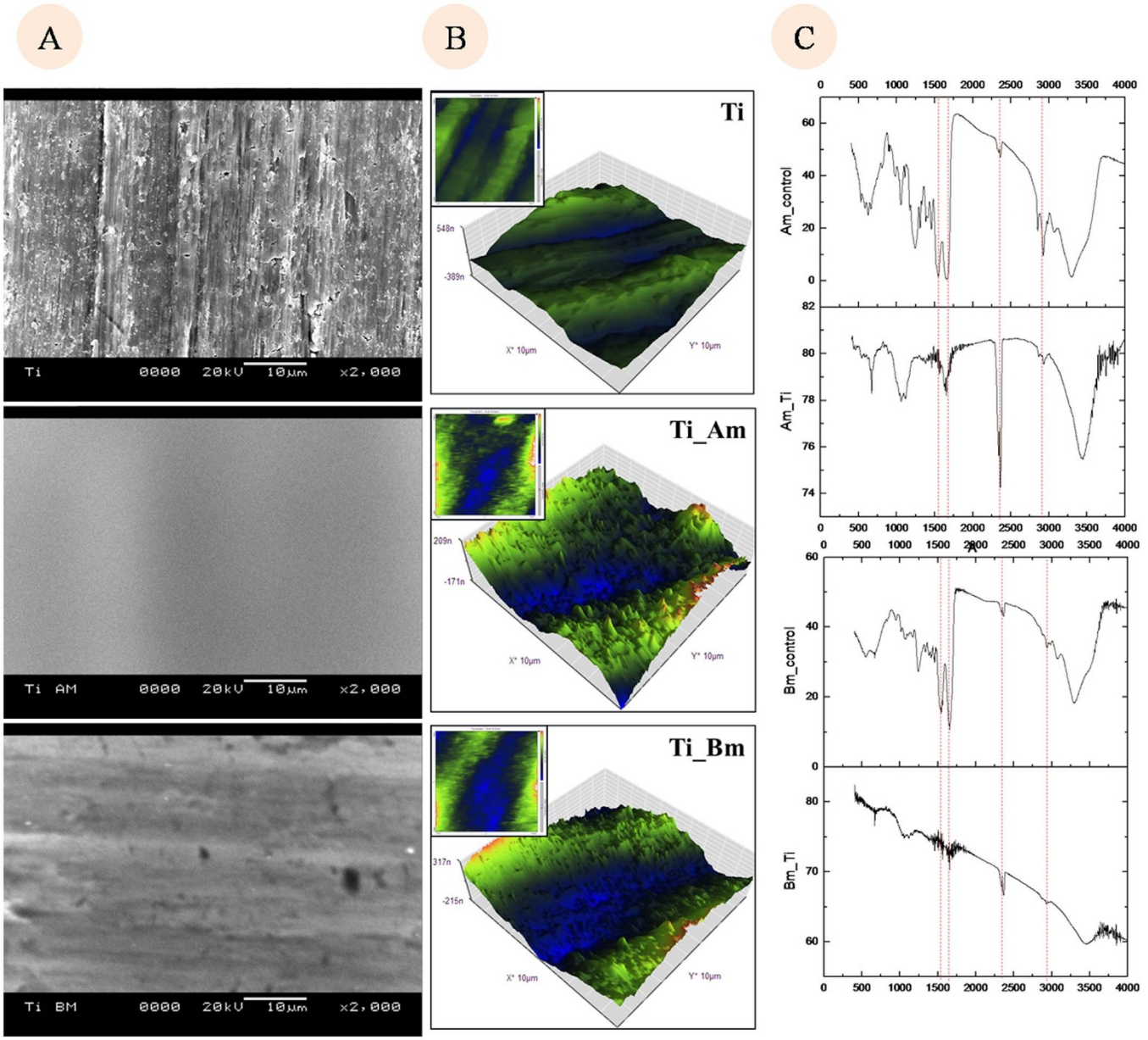

Figure 1 | Surface topography and surface chemistry analysis of protein immobilized titanium. (1A) Scanning electron microscopic image of pristine and fibroin immobilized titanium surface. Protein immobilized Ti coupons are visualized under scanning electron microscope. (1B) Atomic force microscopic image of pristine and fibroin immobilized titanium surface. Protein immobilized Ti are analyzed with non-contact tapping mode of (Veeco, Multimode, Nanoscope-IIIA). Three dimensional image of 10 µm × 10 µm area are represented with 2D image of same region in inset. (1C) FTIR pattern of free and protein immobilized Ti surface. Protein immobilized surface shows distinct transmittance peak at 3100–3300 cm^{-1}, 1600–1700 cm^{-1} and 1510–1580 cm^{-1} (indicated with red dotted lines) in line with free protein, which represents amide A, B, amide I and amide II of protein secondary structure.

Table 1 | Quantification of chemical compositions of pristine and modified Ti surfaces through XPS and EDX

Detection method	Elements	Ti	TiAm	TiBm
XPS	C1s	38.3	60.7	60
	N1s	2.6	10.2	9.8
	O1s	40.3	24.4	41.5
	Ti2p	18.4	1.4	1.5
EDX	CK	ND	66.29	69.33
	TiK	100	6.33	30.67

staining. Non-mulberry fibroin immobilized samples are found to contain maximum amount of calcium nodules in compare to others within day 14 of culture (Fig. 6C).

Discussion

Effective integration of orthopedic implants requires a sequential process of osteoinduction, osteoconduction and osseointegration. Physiochemical nature of the implant surface can be controlled by deposition of biomolecules, which in turn may control the directional cell adhesion and enhanced behavior. Silk protein fibroin of mulberry source is widely used as an effective precursor for fabrication of various matrices. Additionally *B. mori* fibroin is functionalized with RGD sequences for eliciting specific cellular responses

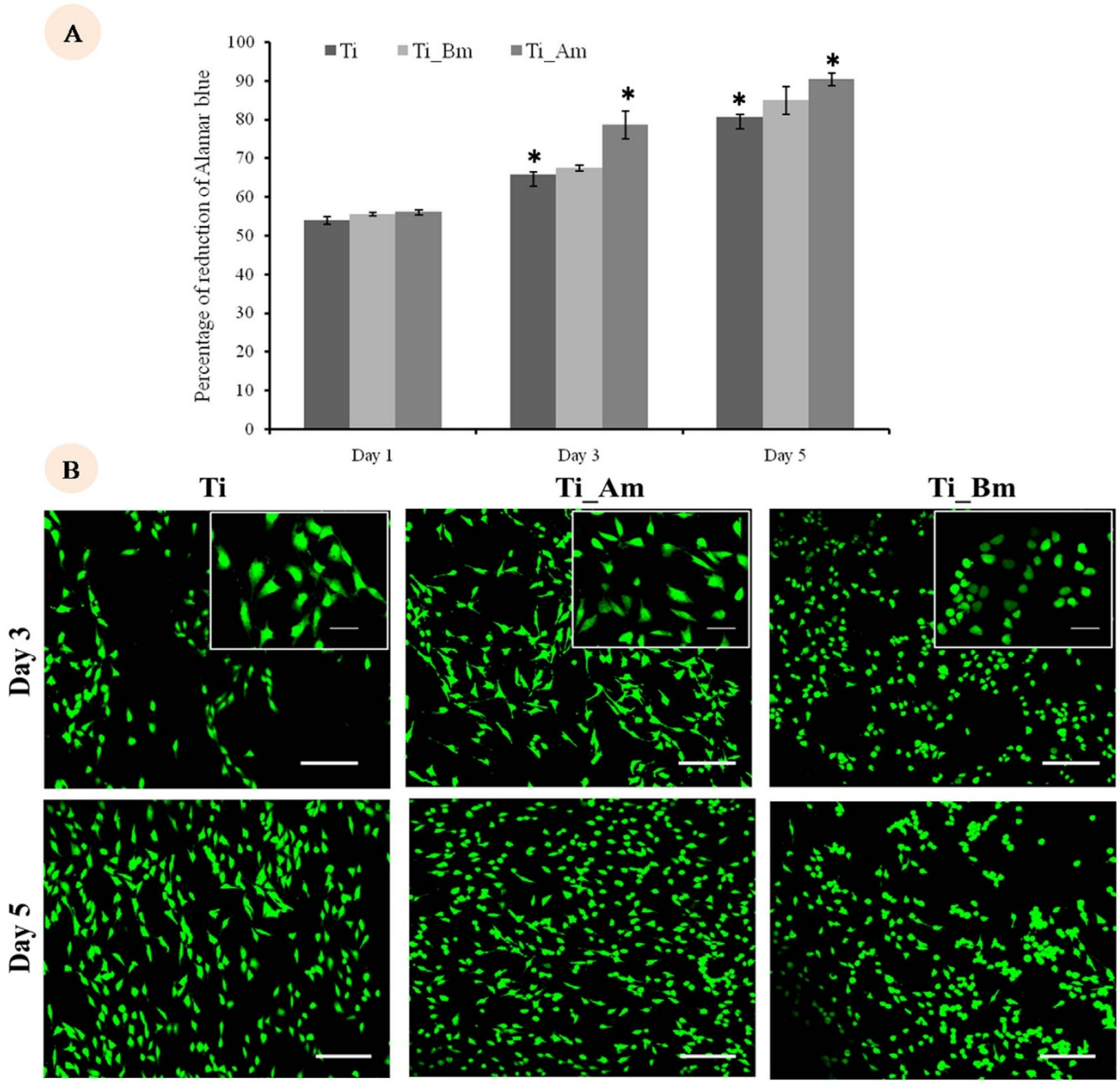

Figure 2 | Analysis of cell proliferation and viability. (2A) Comparative analysis of cell proliferation rate. Osteoblast like cells (MG63) are seeded (1500 cell/cm^2) on Ti surface and cultured for 1, 3 and 5 days. Alamar blue dye was added to each sample and incubated for 4 hrs. Optical density of supernatant is measured at 570 and 600 nm at microplate reader. Statistical analysis of difference of mean was carried out by Student's t-test. * denotes statistically significant difference ($p < 0.05$) between Ti and Am. (2B) Fluorescence image of Live/Dead stained cells. Osteoblast like cells (MG 63) are seeded on Ti surface (1500 cell/cm^2). Cells are stained with Live/Dead stain visualized with CLSM using 10× objective. The cell morphology is analyzed at 40× (inset). Scale bars are 20 μm and 5 μm (inset).

and directing new tissue formation for tissue engineering applications[25,26]. Vidal et al. [2012] report chemically coupled RGD-fibroin complex, while Wohlrab et al. [2012] confirm the superiority of genetically intercalated RGD sequences over chemical coupling. Fibroins originated from non-mulberry silkworms such as *Antheraea mylitta* and *A. pernyi*, etc. are reported as potential biomaterial due to their inherent integrin binding sequences[28–31].

The present report deals with the *in vitro* osteogenic capacity of the silk fibroins immobilized titanium surfaces. The fibroins obtained from non-mulberry (Am) and mulberry (Bm) sources are used to immobilize on the Ti surface. The modified surfaces exhibit significantly altered surface nano-roughness, though the inherent micro-roughness of Ti surface remains mostly unaltered as observed by AFM. The cells of osteoblast-lineage are reportedly able to identify the nanostructure superimposed on micro rough surface and respond to them with a synergistic production of factors related to osteogenic maturation[32]. Thus the local nano-topography of fibroin immobilized surfaces represents a favorable condition for cell adhesion in compare to the pristine Ti. The chemical analysis of modified surfaces is carried out by XPS and EDX, which support the successful immobilization of fibroin molecules as confirmed by increasing content of carbon and nitrogen with a decreasing Ti content. Irreversible immobilization of biomolecules on implant surface is essential to minimize the pH and stress induced loss of such molecules, though it may alter the motifs affecting their functionality. FTIR analysis of immobilized fibroin shows the signature amide I and II peaks while compared with free protein[33]. Uniform deposition of the protein molecules over Ti surface through silane mediated cross-linking creates layers with thickness within sub micron scale[34]. Directional adhesion of osteoblasts to the surface increases the osseo-integrative

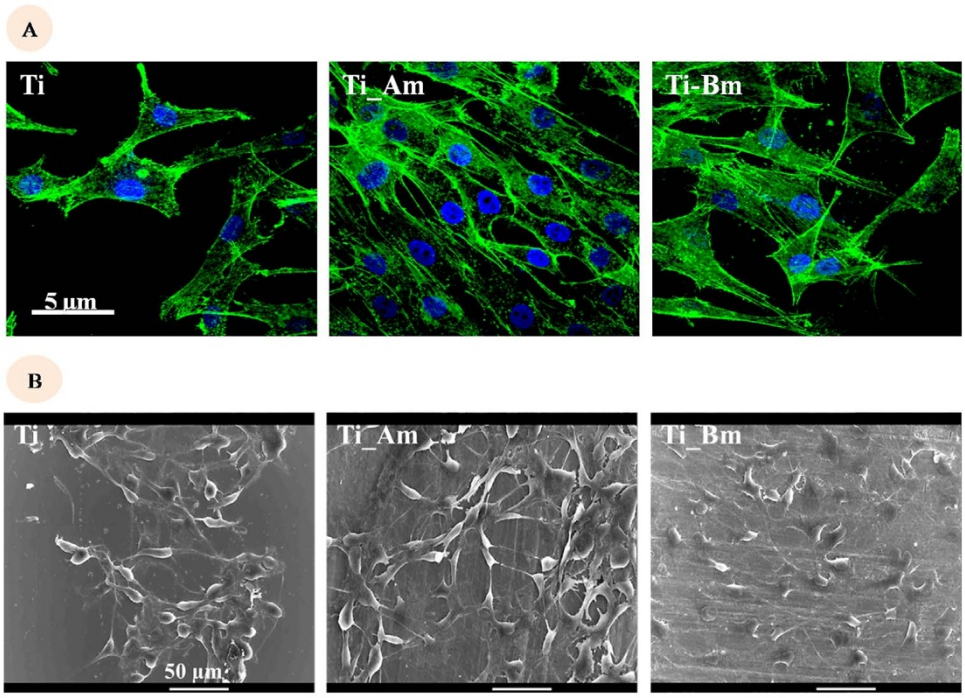

Figure 3 | Analysis of cytoskeleton distribution and cell morphology on titanium surface. (3A) Actin cytoskeleton of osteoblast like cells on pristine and protein immobilized Ti surface. Osteoblast like cells seeded on Ti surfaces are fixed and permeabilized. Actin cytoskeleton and nucleus are stained with FITC conjugated phalloidin (green) and Hoechst 33258 (blue) respectively. Imaging is carried out with CLSM using 488 nm and 405 nm laser. Scale bar is 5 µm. (3B) Scanning electron microscopy of the adhered cells. Osteoblasts like cells are fixed with 4% PFA. Gold sputtering was done after graded dehydration for scanning electron microscopy. Scale bar is 50 µm.

potential of the implant, which involves integrin binding motif such as RGD sequences[25–27]. Non-mulberry fibroin can ideally serve a significant role in initial cell attachment and future proliferation as observed in the initial cell adhesion study. The presence of RGD sequences also influence the focal adhesion complex formation and maturation, which further affect the cell viability and proliferation.

Prior to the formation of their own extra cellular matrices, the cellular behavior and cytoskeleton organization are mostly controlled by the surface chemistry and roughness. The Am fibroin immobilized surface supports the formation of actin stress fiber and moderate cell spreading, which further control other cellular function such differentiation and mineralization. Regular spindle shaped cellular morphology are observed on Am fibroin in comparison to the globular appearance on pristine and Bm fibroin immobilized surface indicating the presence of healthy and viable cells on the prior. To initiate *in vitro* mineralization the differentiation of osteoblast like progenitor cell is necessary. This is investigated by quantifying different osteogenic markers such as osteocalcin and alkaline phosphatase[35]. The fibroin immobilized surface shows significantly higher amount of osteocalcin (OC) and alkaline

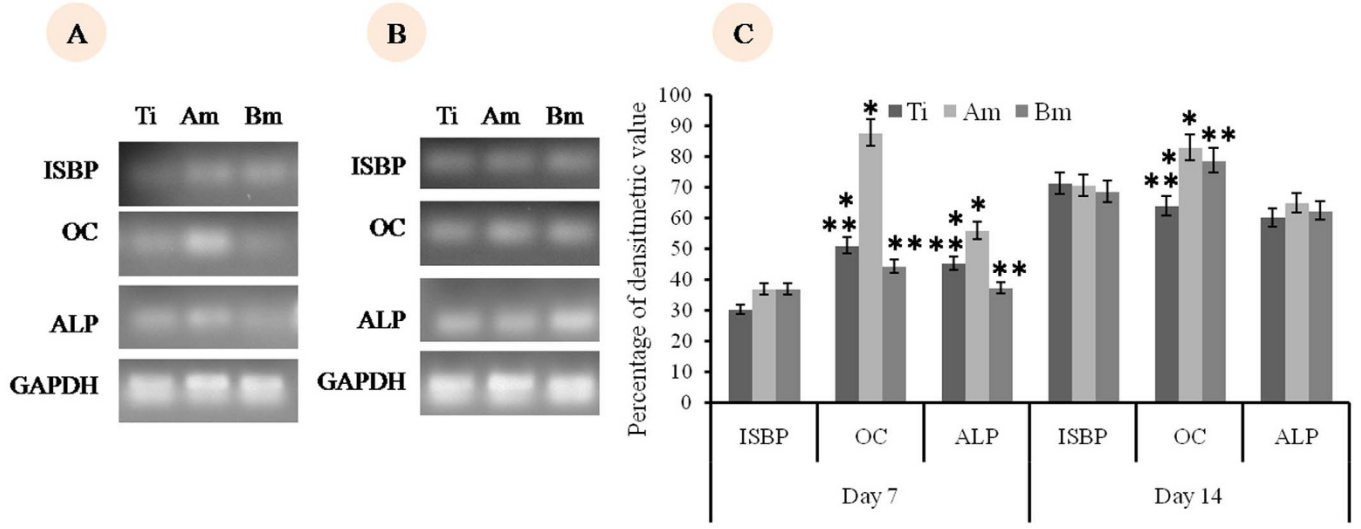

Figure 4 | Osteoblast differentiation. Semi-quantitative RT-PCR of osteoblast differentiation gene markers. End products of semi-quantitative reverse transcription (sqRT-PCR) reaction are analyzed with agarose gel. Densitometric quantification was done from the image of PCR product using ImageJ software and normalized values (with GAPDH as internal control) were plotted. Statistical analysis of mean densitometric values of RT-PCR product was done by Student's t-test. * and ** denotes statistically significant difference ($p < 0.05$) between Ti, Am and Ti and Bm respectively.

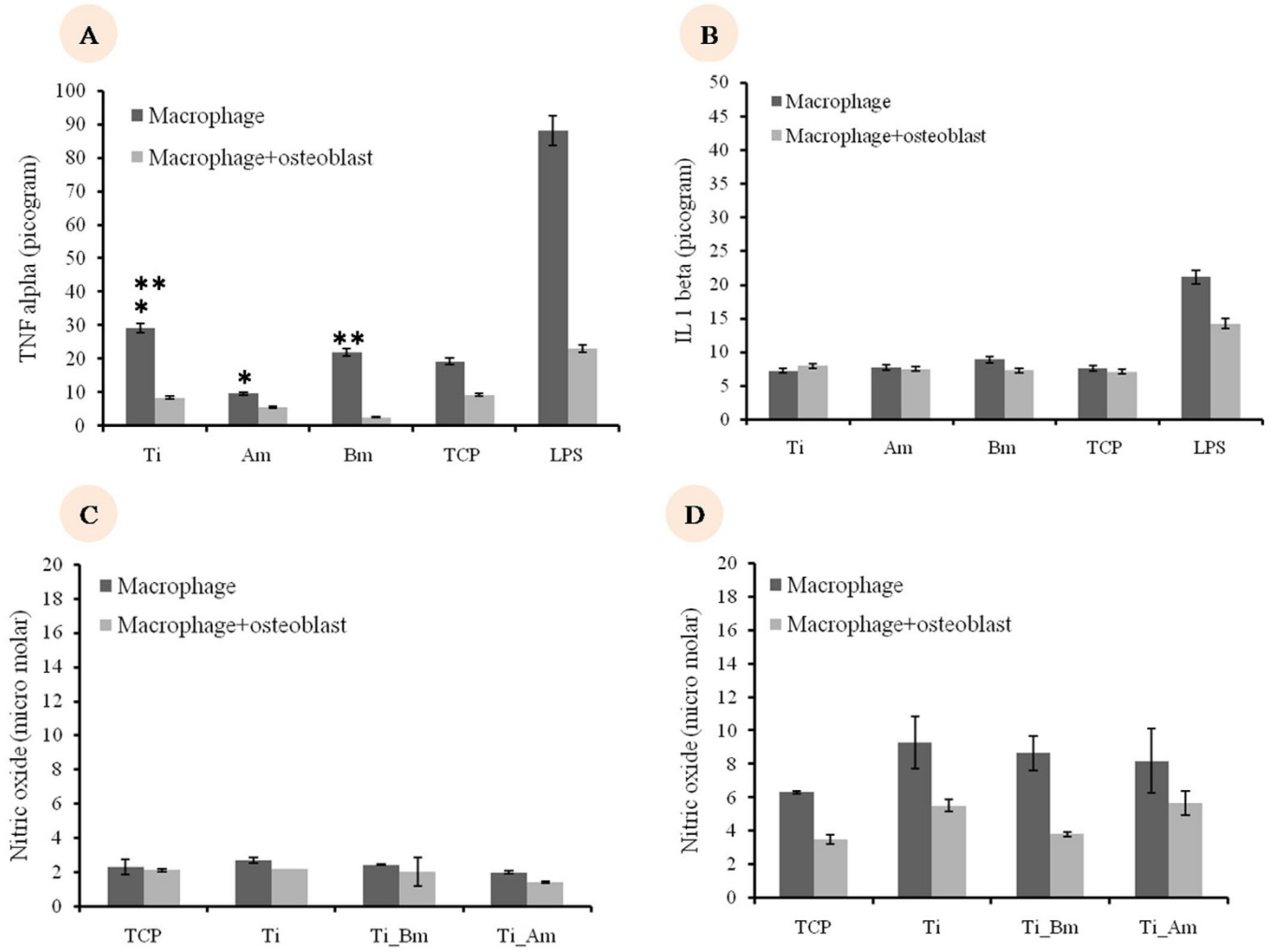

Figure 5 | In vitro inflammatory effect of fibroin coated Ti surfaces. (5A–B) Murine macrophage (Raw 264.1) is cultured with or without osteoblast like cells (MG-63) for 24 hr. Cell supernatant was collected and TNF-α, and IL-1β levels are measured by Quantikine kit (Invitrogen, USA). Product quantity is measured at 450 nm and plotted. (5C–D) Nitric Oxide (NO) level in cell supernatant of 24 and 72 hr are is measured at 450 nm and plotted. Statistical analysis is carried out by Student's T-test. * and ** denote statistically significant difference ($p < 0.05$) between Ti, Am and Bm respectively. No significant differences in IL-1β and NO production are observed between control and experimental samples.

phosphatase (ALP) mRNA in comparison to the pristine Ti on day 7. This supports the influence of nanostructures in osteogenic maturation. The increased amount of OC and ALP in Am fibroin in compare to Bm fibroin, in spite of having similar surface topography. This suggests the superiority of Am fibroin in promoting osseointegration *in vitro*.

Inflammatory responses against the implanted material include an array of cytokines such as TNF-α, IL-1β, M-CSF, etc.[36] which reportedly promote bone resorption and implant failure. The production of nitric oxide also influences osteoblast differentiation. The fibroin immobilized surfaces show significantly low inflammatory response in terms of TNF-α secretion in comparison to pristine Ti, which is in the line with previous reports[2]. Further this supports its candidature as an implant coating material. The recent report shows the influence of bone specific macrophages (osteoMac) on osteogenesis and differentiation during bone development[37]. On the other hand migrating macrophages reach the implanted surface initially and may have an important role in osteoblast adhesion for implant integration. The direct connection between immuonological and ostegogenic system is also demonstrated during pathological conditions such as fracture, where the presence of macrophage and macrophage secreted cytokines controls the bone remodeling. The present study also reports a co-culture model using macrophage and osteoblast to analyze the direct influence of macrophages on osteoblast adhesion and subsequent mineralization. Interestingly the direct co-culture model of macrophage and osteoblast shows much lower level of TNF-α, IL-1β and nitric oxide (NO) production in comparison to macrophage only model, which can be explained by the cellular cross-talk. The influence of macrophages on osteoblast adherence on the Ti surfaces is analyzed microscopically using pre-stained cells. The macrophage does not appear to prevent the adhesion of osteoblast like cells on fibroin embedded surfaces. The osteoblast adhesion is reduced dramatically on pristine Ti surface in co-culture mode. It can be assumed that Am fibroin enhance the macrophage-osteoblast interaction in a synergistic way, without eliciting any detectable immune-response. Subsequent mineralization is also analyzed on co-culture surfaces after long term incubation. It becomes evident that Am fibroin coated surface response more efficiently for calcium nodule formation. Analysis of macrophage mediated effects on osteoblast function warrants more attention in future investigation.

The present report puts forward some important information in relation to the immobilization of silk protein fibroin on Ti surface in terms of the clinical application: (i) Am fibroin immobilization is effective for long term analysis because of the irreversible immobilization and the presence of inherent RGD sequences on fibroin does not require additional cross linking of integrin binding motifs; (ii)

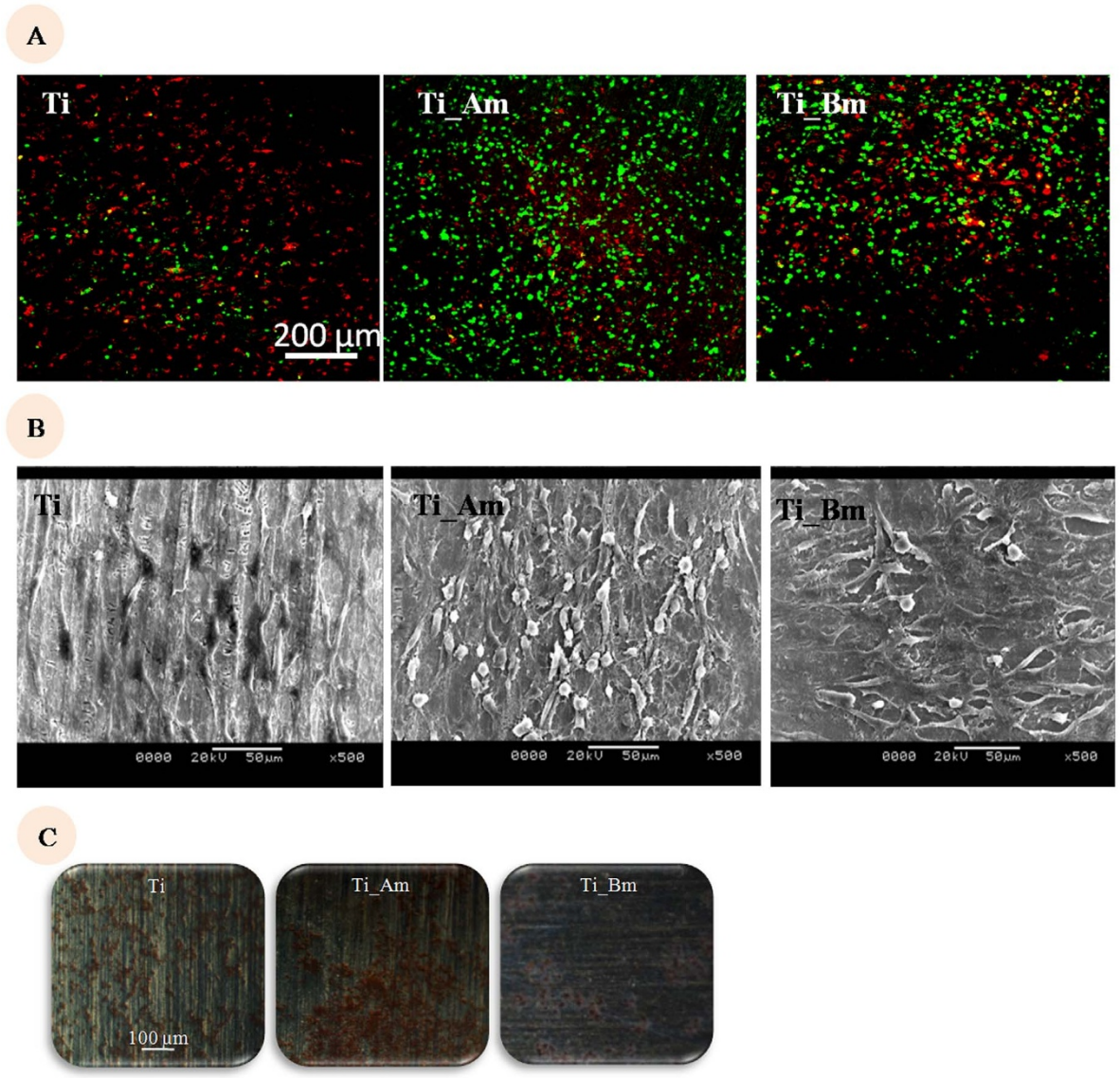

Figure 6 | Effect of macrophage-osteoblast coculture on osteoblast adhesion and function. (6A)-Influence of macrophage, on osteoblast adhesion on Ti surface. Pre-stained macrophage (red) and osteoblast (green) are seeded on pristine and modified Ti surface in 2 : 1 ratio. Imaging with CLSM is done after 24 hr. (6B)-Influence of macrophage, on Osteoblast morphology. Macrophage and osteoblast are seeded on pristine and modified Ti surface and subjected to scanning electron microscopy. Scale bar is 50 µm. (6C)-Calcium deposition on the co-cultured surfaces. Imaging of alizarin red stained co-cultured surfaces is done after 14 days. Scale bar is 100 µm.

The decreased inflammatory response can be useful to reduce the implant mediated immune-response; (iii) The direct interactions between macrophage and osteoblast exhibit enhanced mineralization and (iv) Further investigations are required to define the interactions between macrophage and osteoblast and their impact on the implant acceptance which include *in vivo* investigation.

Conclusion

Titanium, a bio-compatible metal, is widely used for dental and orthopedic implants. Impaired cell adherence and insufficient mineralization on bare metal implants lead to implant failure. In this report the effects of covalently immobilized silk protein fibroin of non-mulberry origin on osteoblast adhesion, proliferation and osteogenic differentiation are analyzed in comparison with the mulberry fibroin. Non-mulberry fibroin exhibits enhanced cell adhesion and mineralization in presence of macrophages without eliciting significant immune-response. This study confirms the candidature of fibroins particularly of Indian tropical non-mulberry tasar origin as a biologically important molecule for implant surface modification.

Methods

Extraction and purification of silk fibroins. Mulberry fibroin was extracted from the silk cocoons of *Bombyx mori* (Bm) obtained from Debra Sericulture Farm, Directorate of Sericulture, West Midnapore, West Bengal, India by the process as described earlier[21,22]. Briefly the Bm cocoons were cut into small pieces and boiled for 30 min in an aqueous solution of 0.02 M Na_2CO_3 for complete degumming and removal of glue silk protein sericin. The fiber pieces were then washed thoroughly in distilled water and dried completely at 50°C. The fibers were dissolved in 9.3 M lithium bromide to get fibroin solution. After centrifugation at 9000 r.p.m for 10 min the supernatant was collected and dialyzed using the cellulose dialysis tubing of MWCO 12 kDa (Pierce, Rockford, IL, USA) for 2 days in room temperature against de-ionized water with frequent changes. The protein was stored at low temperature (−20°C) until further use.

Non-mulberry silk fibroin protein was collected from the posterior silk glands of live matured fifth instar larvae of Indian tropical tasar silkworm *Antheraea mylitta* (Am) obtained from Taldangra Tasar Farm, Bankura District and IIT Kharagpur Biotechnology Farm, West Bengal, India. Silk gland extracted water insoluble protein

fibroin was solubilized with 1% sodium lauryl sulfate (SLS)[30,31]. The solubilized fibroin was dialyzed for 10–12 hrs at room temperature against deionized water with frequent changes. The fibroin solution was stored at −20°C. Protein content was estimated by colorimetric (Bradford) method.

Modification of titanium (Ti) surface. *Silanization of Ti surface using APTES.* The titanium sheet (0.1 mm thickness with 99.9% purity from Sigma Aldrich, St Louis, USA) was cut into 1 cm × 1 cm pieces. The pieces were then washed thoroughly for 15 min each by sonication in acetone (70% v/v) followed by ethanol and de-ionized water. The samples were dried to facilitate the silanization process. The immobilization of APTES (Sigma Aldrich, St Louis, USA) on the titanium samples was carried out by following the recipes mentioned earlier[28] with little modifications. The cleaned pieces were submerged in a 2% (v/v) solution of APTES in toluene for 10 h at room temperature. The samples were washed with pure toluene thrice (each 30 min) to remove any residual APTES. To remove the toluene, the metal pieces were washed with ethanol followed by deionized water. Gluteraldehyde solution (2%) (Sigma Aldrich, St Louis, USA) was poured over the Ti-APTES samples and left for 5 h at room temperature. The samples were further rinsed thoroughly with deionized water and dried.

Immobilization fibroins of mulberry (Bm) and non-mulberry (Am) origins. Bm and Am fibroin solutions (each 20 mg/ml) in PBS were used for immobilization. The silanized Ti samples were incubated in the protein solution for 60 min at 25°C. After the immobilization the metal pieces were washed thrice in distilled water to remove any unattached fibroin.

Cell culture and maintenance. Mouse osteoblast cell line (MG-63) and mouse macrophage (RAW 264.7) cells were cultured in Dulbecco's Modified Eagle's Medium (Invitrogen, USA) supplemented with 10% fetal bovine serum, 100 U/ml penicillin and 100 mg/ml streptomycin (Gibco BRL, Grand Island, NY, USA). All the cell lines were incubated at 37°C in a humidified atmosphere of 5% CO_2 with the growth media changed every 48 h. The subsequent passages were carried out from the confluent monolayer of cells obtained by washing the cells with sterile 1× phosphate buffered saline (PBS) pH 7.4 and trypsinization with chilled 1× trypsin EDTA (Gibco BRL Grand Island, NY, USA). The harvested cells were centrifuged and seeded on Ti surface (1500 cell/cm^2) for further experimentation.

Analysis of the modified surface topography. *Surface morphology analysis by SEM.* The surface morphology of pristine Ti, and modified Ti samples were observed after gold sputtering using SEM (JEOL JSM 5800).

Surface topography analysis by AFM. AFM (Veeco, Multimode, Nanoscope-IIIA) was carried out by scanning the 10 × 10 μm^2 area in non-contact mode with tips mounted on cantilevers at spring constant of 40 N/m (as specified by the manufacturer). Quadric roughness was calculated to compare the surface roughness of control and experimental samples.

Analysis of modified surface chemistry. *XPS and EDX analysis.* The chemical composition of pristine Ti, and modified samples were determined by XPS (PHI 5000 Versa Probe III, Physical Electronics, Inc. Minnesota, USA) and EDX (INCA Penta FET ×3, Oxford Instrument UK).

FTIR analysis. The infrared absorption spectra of the free protein and the protein immobilized samples were obtained from an FTIR spectrophotometer (Shimadzu DT-40 model 883 IR Spectrophotometer) in diffuse reflectance mode. For each spectrum obtained, a total of 64 scans were accumulated at 4 cm^{-1} resolution. Scanning was conducted in the range from 400 to 4000 cm^{-1}.

Analysis of osteoblast like cell adherence, proliferation/viability and morphology. *Cell proliferation.* MG-63 cells were seeded at a density of 1500 cells/cm^2 on pristine Ti and coated Ti samples and cultured at 37°C in a humidified atmosphere with 5% CO_2. The cell seeded samples were washed in sterile 1× PBS and placed into fresh sterile wells after 1, 3 and 5 days. Alamar blue (Resazurin) dye (Invitrogen, USA) was used following Manufacturer's protocol and dye reduction was measured by measuring optical density of the solution at 570 and 600 nm.

Cell viability. The cell seeded surfaces were rinsed three times with sterile 1× PBS carefully and incubated with live/dead stain (Molecular Probes, Invitrogen, USA) for 30 min at room temperature. Live/dead stained cells were visualized under confocal microscope (CLSM) using 488 and 564 nm lasers (Fluoview1000, Olympus, Japan).

Analysis of cytoskeleton organization and cellular morphology. For actin filament staining, the cell seeded Ti coupons were fixed with 2% PFA and permeabilized with 0.1% TritonX-100. FITC conjugated phalloidin (actin) and Hoechst (nucleus) were used in 1 : 200 dilution (in 1× PBS). The samples were analyzed using 405 nm and 488 nm laser in CLSM.

To analyze the cell morphology, the cell seeded Ti samples were fixed and prepared for SEM analysis by gradual dehydration. The samples were then gold sputtered and analyzed using SEM.

Analysis of cellular functionality. *RT-PCR analysis.* The cell seeded Ti coupons were treated with Trizol (Invitrogen, USA) followed by the isolation of total RNA using RNA isolation kit (Qiagen, Germany). First strand cDNA was synthesized from 10 μg of total RNA using first strand cDNA synthesis kit (Fermentas, Canada). Semi-quantitative RT-PCR reaction of integrin-binding sialoprotein (IBSP), osteocalcin (OC) and alkaline phosphatase (ALP) were carried out by using custom made forward and reverse primers. Comparative analysis of end products (approx. 120–150 kDa) was performed using gel analysis plug-in of ImageJ software and normalized with GAPDH.

Analysis of immune response elicited by the modified Ti surfaces. *Quantification of TNF-α and IL-1β production from macrophage culture.* Macrophage (10^5 cells/cm^2) cells were seeded on the fibroin coated samples. After 24 h of cell seeding, the complete medium was replaced with incomplete medium. After 24 h supernatant was collected to analyze TNF-α and IL-1β level using TNF-α and IL-1β quantification kit (Invitrogen, USA). Nitric oxide level was analyzed with samples from 24 hr and 72 hr, using Griess reagent (Sigma, St Louis, USA). The data accumulations were carried out at 450 nm and 600 nm using a microplate reader.

Analysis of macrophage elicited influence on osteoblast activity. *Osteoblast adhesion in macrophage-osteoblast co-culture.* For direct co-culture the osteoblast (0.5 × 10^5/cm^2) and macrophage (10^5 cells/cm^2) cells were pre-stained with CellTracker™ Green CMFDA (Invitrogen) and CellTracker™ Orange CMTMR (Invitrogen) respectively for 30 min following the Manufacturer's protocol. Cell seeded surfaces were treated as per standard protocol and fixed with 2% PFA. Imaging was carried out using 488 and 543 nm laser in CLSM (FV1000, Olympus, Japan) in sequential mode to analyze the cell adhesion efficiency.

Adhered cell morphology in co-culture model was analyzed by fixing the surface with 2% PFA and prepared for SEM analysis by gradual dehydration. The samples were then gold sputtered and analyzed using SEM (JEOL JSM 5800).

Quantification of TNF-α, IL-1β and nitric oxide (NO) production in macrophage-osteoblast co-culture. The macrophage and osteoblast cells (2 : 1 ratio) were seeded on pristine and modified Ti for 24 hr. The cell supernatants were collected and analyzed for TNF-α, IL-1β and NO quantifications as stated before.

Calcium deposition. Alizarin red staining for mineralization was performed after fourteen days of co-culture. The cell seeded samples were fixed with 10% formalin, and stained in 1% alizarin red S (Sigma Aldrich, St Louis, USA) solution (pH 4.0) for 8–10 min. Images were taken with ECLIPSE TS100 (Nikon, Japan).

Statistical analysis. All the experiments were repeated three times (with sample number ≥3) and the mean value are plotted with standard deviations. The statistical significance is calculated using Student's t test.

1. Brunette, D. M. (ed.) Titanium in Medicine. (Springer-Verlag, Berlin & Heidelberg. 2001).
2. Horowitz, S. M. & Gonzales, J. B. Inflammatory Response to Implant Particulates in a Macrophage/Osteoblast Coculture Model. *Calcif. Tissue Int.* **59**, 392–396 (1996).
3. Schierholz, J. M. & Beuth, J. Implant infections: a haven for opportunistic bacteria. *J. Hosp. Infect.* **49**, 87–93 (2001).
4. Sul, Y. *et al.* Characteristics of the surface oxides on turned and electrochemically oxidized pure titanium implants up to dielectric breakdown: the oxide thickness, micropore configurations, surface roughness, crystal structure and chemical composition. *Biomaterials* **23**, 491–501 (2002).
5. Albrektsson, T. & Johanssen, C. Osteoinduction, osteoconduction and osseointegration. *Eur. Spine. J.* **10**, 96–101 (2001).
6. Yamamoto, D. *et al.* Osteoconductivity and hydrophilicity of TiO_2 coatings on Ti substrates prepared by different oxidizing processes. *Bioinorg. Chem. Appl.* **2012**, 1–7 (2012).
7. Han, C. M., Lee, E. J., Kim, H. E., Koh, Y. H. & Jang, J. H. Porous TiO_2 films on Ti implants for controlled release of tetracycline-hydrochloride (TCH). *Thin Solid Films* **519**, 8074–8076 (2011).
8. Vallés, G., Gil-Garay, E., Munuera, L. & Vilaboa, N. Modulation of the cross-talk between macrophages and osteoblasts by titanium-based particles. *Biomaterials* **29**, 2326–2335 (2008).
9. Chen, H. T. *et al.* Osteoblast growth behavior on micro-arc oxidized β-titanium alloy. *Surf. Coat. Tech.* **205**, 1624–1629 (2010).
10. Faeda, R. S., Tavares, H. S., Sartori, R., Guastaldi, A. C. & Marcantonio, E., Jr. Evaluation of titanium implants with surface modification by laser beam: biomechanical study in rabbit tibias. *Braz. Oral. Res.* **23**, 137–143 (2009).
11. Piattelli, A., Scarano, A., Piattelli, M. & Calabrese, L. Direct bone formation on sand-blasted titanium implants: an experimental study. *Biomaterials* **17**, 1015–1018 (1996).
12. Guehennec, L. L., Soueidan, A., Layrolle, P. & Amouriq, Y. Surface treatments of titanium dental implants for rapid osseointegration. *Dent. Mater.* **23**, 844–854 (2007).
13. Ball, M. D. *et al.* Osteoblast growth on titanium foils coated with hydroxyapatite by pulsed laser ablation. *Biomaterials* **22**, 337–347 (2001).
14. Rupp, F. *et al.* Enhancing surface free energy and hydrophilicity through chemical modification of microstructured titanium implant surfaces. *J. Biomed. Mater. Res. A* **76**, 323–334 (2006).

15. Leedy, M. R. *et al.* Use of chitosan as a bioactive implant coating for bone-implant applications. *Adv. Polym. Sci.* **244**, 129–165 (2011).
16. Giannoni, P. *et al.* Osteogenic differentiation of human mesenchymal stromal cells on surface-modified titanium alloys for orthopedic and dental implants. *Int. J. Artif. Organs* **32**, 811–820 (2009).
17. Morra, M. Biochemical modification of titanium surfaces: peptides and ECM proteins. *Eur. Cell Mater.* **12**, 1–15 (2006).
18. Kashiwagi, K., Tsuji, T. & Shiba, K. Directional BMP-2 for functionalization of titanium surfaces. *Biomaterials* **30**, 1166–1175 (2009).
19. Degasne, I. *et al.* Effects of roughness, fibronectin and vitronectin on attachment, spreading, and proliferation of human osteoblast-like cells (Saos-2) on titanium surfaces. *Calcif. Tissue Int.* **64**, 499–507 (1999).
20. Pallu, S. *et al.* The effect of cyclo-DfKRG peptide immobilization on titanium on the adhesion and differentiation of human osteoprogenitor cells. *Biomaterials* **26**, 6932–6940 (2005).
21. Omenetto, F. G. & Kaplan, D. L. New Opportunities for an ancient material. *Science* **329**, 528–531 (2010).
22. Rockwood, D. N. *et al.* Materials fabrication from *Bombyx mori* silk fibroin. *Nat. Protoc.* **6**, 1612–1631 (2011).
23. Sofia, S., McCarthy, M. B., Gronowicz, G. & Kaplan, D. L. Functionalized silk-based biomaterials for bone formation. *J. Biomed. Mater. Res.* **54**, 139–148 (2001).
24. Bhumiratana, S. *et al.* Nucleation and growth of mineralized bone matrix on silk-hydroxyapatite composite scaffolds. *Biomaterials* **32**, 2812–2820 (2011).
25. Vidal, G. *et al.* Enhanced cellular adhesion on titanium by silk functionalized with titanium binding and RGD peptides. *Acta Biomater.* **9**, 4935–4943 (2012).
26. Wohlrab, S. *et al.* Cell adhesion and proliferation on RGD-modified recombinant spider silk proteins. *Biomaterials* **33**, 6650–6659 (2012).
27. Nayak, S., Dey, T., Naskar, D. & Kundu, S. C. The promotion of osseointegration of titanium surfaces by coating with silk protein sericin. *Biomaterials* **34**(12), 2855–2864 (2013). (DOI: 10.1016/j.biomaterials.2013.01.019. Epub 2013 Jan 26.)
28. Kundu, S. C. *et al.* Nonmulberry silk biopolymers. *Biopolymers* **97**, 455–467 (2012).
29. Patra, C. *et al.* Silk protein fibroin from *Antheraea mylitta* for cardiac tissue engineering. *Biomaterials* **33**, 2673–2680 (2012).
30. Mandal, B. B. & Kundu, S. C. Osteogenic and adipogenic differentiation of rat bone marrow cells on non-mulberry and mulberry silk gland fibroin 3D scaffolds. *Biomaterials* **30**, 5019–5030 (2009).
31. Datta, A., Ghosh, A. K. & Kundu, S. C. Purification and characterization of fibroin from the tropical saturniid silkworm, *Antheraea mylitta*. *Insect Biochem. Mol. Biol.* **31**, 1013–1018 (2001).
32. Gittens, R. A. *et al.* Differential responses of osteoblast lineage cells to nanotopographically-modified, microroughened titanium-aluminum-vanadium alloy surfaces. *Biomaterials* **33**, 8986–8994 (2012).
33. Acharya, C., Ghosh, S. K. & Kundu, S. C. Silk fibroin film from non-mulberry tropical tasar silkworms: A novel substrate for in vitro fibroblast culture. *Acta Biomaterialia.* **5**, 429–437 (2009).
34. Kato, K., Uchida, E., Kang, E. T., Uyama, Y. & Ikada, Y. Polymer surface with graft chains. *Prog Polym Sci* **28**, 209–259 (2003).
35. Kim, S. E. *et al.* The effect of immobilization of heparin and bone morphogenic protein-2 (BMP-2) to titanium surfaces on inflammation and osteoblast function. *Biomaterials* **32**, 366-373 (2011).
36. Chaudhary, L. R., Spelsberg, T. C. & Riggs, B. L. Production of various cytokines by normal human osteoblast-like cells in response to interleukin-1 beta and tumor necrosis factor-alpha: lack of regulation by 17-beta-estradiol. *Endocrinology* **130**, 2528–2534 (1992).
37. Arron, J. R. & Choi, Y. Osteoimmunology: Bone versus immune system. *Nature* **408**, 535–536 (2000).

Acknowledgments

This work is supported by Department of Biotechnology, and Department of Science and Technology, Government of India. We are greatly indebted to Dr. Mahitosh Mandal and Dr. Ananta K. Ghosh, Indian Institute of Technology Kharagpur for scientific inputs and suggestions.

Author contributions

S.C.K. and T.D. design the experiments; D.N., T.D. and S.N. perform the experiments and analyzed the data. D.N., T.D. and S.C.K. wrote the manuscript. The manuscript was written through the contributions of all authors. All authors have given approval to the final version of the manuscript.

Additional information

Supplementary information accompanies this paper at http://www.nature.com/scientificreports

Competing financial interests: The authors declare no competing financial interests.

How to cite this article: Naskar, D., Nayak, S., Dey, T. & Kundu, S.C. Non-mulberry silk fibroin influence osteogenesis and osteoblast-macrophage cross talk on titanium based surface. *Sci. Rep.* **4**, 4745; DOI:10.1038/srep04745 (2014).